Design of Mechanical Properties of Poly(butylene-adipate-terephthalate) Reinforced with Zein-TiO2 Complex

Hindawi
Material Design & Processing Communications
Volume 2022, Article ID 6496985, 10 pages
https://doi.org/10.1155/2022/6496985

Research Article

Design of Mechanical Properties of Poly(butylene-adipate-terephthalate) Reinforced with Zein-TiO_2 Complex

Elena Togliatti,[1] **Maria Grimaldi**,[2] **Olimpia Pitirollo**,[2] **Antonella Cavazza**,[2] **Diego Pugliese**,[3] **Daniel Milanese**,[1] **and Corrado Sciancalepore**[1]

[1]*Dipartimento di Ingegneria e Architettura (DIA) and INSTM RU, Università di Parma, Parco Area delle Scienze 181/A, 43124 Parma, Italy*
[2]*Dipartimento di Scienze Chimiche, Della Vita e della Sostenibilità Ambientale (SCVSA), Università di Parma, Parco Area delle Scienze 17/A, 43124 Parma, Italy*
[3]*Dipartimento di Scienza Applicata e Tecnologia (DISAT) and INSTM RU, Corso Duca degli Abruzzi 24, 10129 Torino, Italy*

Correspondence should be addressed to Corrado Sciancalepore; corrado.sciancalepore@unipr.it

Received 5 March 2022; Revised 12 June 2022; Accepted 28 June 2022; Published 20 July 2022

Academic Editor: Guian Qian

Mechanical properties of polymer biocomposites are influenced by the interaction between the matrix and the filler surface. In this work, composites based on poly(butylene-adipate-terephthalate) (PBAT) filled with micrometric particles of zein-TiO_2 complex (ZTC) were realized via solvent casting technique at different concentrations, equal to 0, 5, 10, and 20 wt%. After pelletization, the resulting materials were injection molded into standard specimens, employed for the uniaxial tensile test (UTT) characterization. From the stress-strain curves, Young's modulus (E), yield stress (σ_y), stress at break (σ_B), elongation at break (ε_B), and toughness (T) were collected. The addition of the ZTC proved to show a reinforcing effect on the polymeric matrix, with an increase in both E and σ_y. Modelling of the mechanical properties was performed by applying Kerner's and Pukánszky's equations. Kerner's model, applied on experimental E values, returned a very good correspondence between collected and theoretical values. From the application of Pukánszky's model to σ_y, the obtained B value showed a good interfacial interaction between the matrix and the filler. Due to the enhanced stiffness of the composites, a reduction in the true stress at break ($\sigma_{T,B}$) was observed. The modified Pukánszky's model gave a B value lower than the one obtained for the yield, but still in the range of acceptable values for microcomposites.

1. Introduction

Composite materials have been developed and widely studied in the last decades, because they allow to modify the properties of the pristine matrix, tailoring them to the needs, and to reduce the costs [1].

Poly(butylene-adipate-terephthalate) (PBAT) is one of the most promising polymers in the category of biodegradable materials. PBAT is a random copolyester obtained from fossil resources but characterized by complete biodegradability [2], beside high flexibility and toughness, and mechanical properties comparable to the low-density polyethylene (LDPE) [3].

Several types of fillers, both organic and inorganic, are used as reinforcement for polymer matrix composites. Inorganic fillers include $CaCO_3$, clays, layered silicates, and glass beads, while among the organic ones, wood-based and lignocellulosic materials are the most often employed, thanks to their large availability, natural origin, lightweight, and low cost [4]. In recent years, to improve sustainability of the final products, new filler materials have been obtained as by-products from the agri-food chain scraps, like almonds shells and rice husk, vegetable peels, coffee grounds, egg-, and seafood shells [5–8]. Zein is a prolamin protein derived from corn, studied since the early 20th century [9] and used for the realization of edible films and coatings, but it is difficult to process due to its poor mechanical properties [10].

Recently, titanium dioxide (TiO_2) has been employed as a reinforcing agent in the realization of hybrid inorganic-organic compounds with improved physical and chemical

properties [11]. TiO_2 is an amphoteric, inert, nontoxic, and biocompatible metal oxide, widely used as white pigment additive (E171) in food industry [11] and as an UV-blocking reinforcement phase in food packaging films [12]. The reinforcement of zein films with TiO_2 particles proved to be successful, as obtained by Kadam et al. [13].

Since the addition of a second or even third phase modifies the tensile properties of the matrix it is added to, interphase interactions are an important factor influencing the overall properties of the composite and studying the relationship between the components is of great interest. The best performing composites are obtained when good interphase is created between the matrix and the surface of the filler particles. By considering the properties of composites as a combination of the properties of matrix and filler, many theoretical models have developed relationships between the composite tensile properties and the volumetric fraction of the reinforcing phase. For this work, the detailed and comprehensive publications of Lewis and Nielsen [14, 15], Százdi et al. [16], Pukánszky [17, 18], and Móczó and Pukánszky [1] have been taken as references for the description of the composite mechanical characteristics. The most diffused theories for modelling composite properties are represented by Halpin-Tsai's [19] and Kerner-Nielsen's [14, 20] models as far as elastic modulus is concerned, and by Pukánszky's [18] model regarding tensile strength and interfacial adhesion goodness. Starting from aforementioned ones and adding system-specific considerations to obtain the best fitting, other specific models were developed. For example, new multiple-components models for estimation of elastic modulus were proposed [21], or the influence of carbon nanotubes (CNTs) aspect ratio on the parameter defining the strength of interaction was obtained [22], considering interfacial shear strength as dependent on the interface stress transfer and combining that with Pukánszky's model. Another example can be represented by the development of models for ternary composites, modifying Kerner-Nielsen's and Pukánszky's hypothesis in order to predict tensile modulus of polypropylene (PP)/nanoclay/calcium carbonate ($CaCO_3$) composites and the properties at interphase of PP/montmorillonite/$CaCO_3$, respectively [23, 24].

In this work, zein and TiO_2 were employed to produce a zein-TiO_2 complex (ZTC) to be used as reinforcing phase at different loadings in new sustainable composite materials based on PBAT matrix. The goal of this study is to characterize the mechanical properties of the realized composites and to assess the effectiveness of the reinforcement, analyzing the predictability of properties modification and the interaction between the two phases through the application of Kerner's and Pukánszky's models.

2. Materials and Methods

2.1. Materials. PBAT was purchased in the commercial pellet form from MAgMa Spa (Chieti, Italy) and used without any preliminary operations. Commercial corn zein was purchased from Merck-Sigma (Darmstadt, Germany), and TiO_2 was purchased in the rutile form Carlo Erba reagents (Milan, Italy).

The ZTC complex was prepared with a composition of 1 : 1 of zein to TiO_2. Zein was first dissolved in ethanol (EtOH—Sigma-Aldrich, St. Louis, MO, USA) at 50°C, then TiO_2 was added under constant stirring, until the solution became white and homogeneous. The solution was therefore cast and dried in an oven at 60°C for 16 h to allow complete evaporation of the solvent. Once obtained, the thin film was ground by a planetary mill (Pulverisette 0, Fritsch, Idar-Oberstein, Germany) to achieve a fine powder and finally sifted (stainless steel sieve, Giuliani Technology Srl, Turin, Italy) to a size below 25 μm.

The PBAT-ZTC composites were obtained trought a solvent casting method following three main steps. First, the PBAT was dissolved in chloroform ($CHCl_3$—Sigma-Aldrich, St. Louis, MO, USA) by means of a magnetic stirrer for few hours and the ZTC powder dispersed in the same solvent in a separate container with the same method. The polymer solution and the filler suspension were then mixed to obtain a homogeneous phase that was cast and spread onto a non-stick surface to ensure a small thickness and allow the easy evaporation of the solvent. Lastly, after 12 h under an extractor hood, the film was removed from the surface, manually reduced to pellets, and desiccated at 80°C up to constant mass to eliminate any solvent residues. The composites were realized at four different concentrations: 0, 5, 10, and 20 wt% that were named PBAT, PBAT+5% ZTC, PBAT+10% ZTC, and PBAT+20% ZTC, respectively.

The pellets obtained from this process were utilized for the injection molding of standard specimens (UNI EN ISO 527), through a MegaTech H7/18-1 machine (TECNICA DUEBI Srl, Italy), for mechanical characterization.

2.2. Tensile Test. To carry out the UTT, a TesT dynamometer (Model 112, TesT GMBH Universal Testing Machine, Germany) was employed. The specimens were locked at both ends and subjected to a constant tensile speed of 100 mm/min up to failure. The test was repeated on at least seven specimens for each composite material.

From the stress-strain curves, averaged values of Young's Modulus (E), yield stress (σ_y), stress at break (σ_B), elongation at break (ε_B), and toughness (T) were calculated.

2.3. Composite Modelling. Reinforcing agents and the polymeric structure often create interactions of different nature, given their different chemical structure. It is therefore essential to understand and predict how and in what amount the addition of the fillers affects the properties of the matrix.

2.4. Tensile Modulus. Halpin developed a simplified model to predict the elastic modulus in composites filled with short fibers [25]. The model assumes that the fibers are aligned and oriented parallel or perpendicular to the direction of the stress applied, and the elastic moduli of the composites in the two cases are expressed by E_I in Equation (1) and E_L in Equation (2), respectively, [26]:

$$E_I = E_m\left(1 - \varphi_f\right) + E_p\varphi_f, \quad (1)$$

$$E_L = E_m \left[\frac{1 + \xi \beta \varphi_f}{1 - \beta \varphi_f} \right], \quad (2)$$

where E_p and E_m are, respectively, the filler and matrix moduli, φ_f is the volumetric fraction of the filler, and the parameter ξ represents the particles aspect ratio. β is a parameter defined as $\beta = [(E_p/E_m) - 1]/[(E_p/E_m) + \xi]$.

A similar model was developed by Kerner, who extensively studied elastic properties of composite materials [20]. Kerner's equation can be expressed in the form of the following equation [15]:

$$\frac{E'}{E_0'} = \frac{\left(1 + AC\varphi_f\right)}{\left(1 - C\varphi_f\right)}, \quad (3)$$

where $E^{'}$ and E_0' are the elastic moduli of the composite and matrix, respectively; φ_f is the volumetric fraction of the filler phase; $A = (7 - 5\upsilon)/(8 - 10\upsilon)$ considers the spherical geometry of the filler and the Poisson ratio ν of the matrix; C is defined, analogously to the former β parameter, as $C = [(E_p/E_m) - 1]/[(E_p/E_m) + A]$ and takes into account the relative elastic moduli of the phases.

Lewis and Nielsen [14, 15] modified Kerner's model, pointing out that important factors, like the packing of the filler particles ψ, were neglected. ψ formulation is given as a function of φ_f and the maximum packing factor of the filler φ_m: $\psi = 1 + \varphi_f \bullet [(1 - \varphi_m)/(\varphi_m^2)]$.

Generalized Kerner's equation was then proposed such as in the following equation:

$$\frac{E'}{E_0'} = \frac{\left(1 + AC\varphi_f\right)}{\left(1 - \psi C\varphi_f\right)}. \quad (4)$$

Generally, an increase in stiffness is expected when a matrix is filled with a reinforcing agent.

For this work, modelling of Young's modulus was made applying generalized Kerner's model (Equation (4)) to compare experimental values obtained from the mechanical analysis with predicted calculated values.

φ_f was calculated as $\varphi_f = (g_f/\rho_f)/[(g_f/\rho_f) + (g_m/\rho_m)]$ (with ρ_f and ρ_m the experimental values of the filler and the matrix), and ψ was calculated considering φ_m equal to 0.632 (randomly close packed nonagglomerated spherical particles). υ had been experimentally calculated to be 0.46 by means of noncontact optical digital image correlation (DIC) technique. The modulus of the ZTC was experimentally calculated by dynamic mechanical analysis (DMA).

Table 1 summarizes the values of the parameters used for the application of Kerner's model.

The values of E'/E_0' calculated with Equation (4) were plotted against the volumetric fraction of the filler and overplotted with the experimental values of relative moduli, expressed as the ratio between the moduli of the composite and the matrix.

Table 1: Values of material parameters used in Kerner's equation.

Parameter	Value	Method
E_m	92 MPa	Experimental by UTT
E_p	3900 MPa	Experimental by DMA
ρ_m	1.26 g/cm^3	Tabulated in PBAT datasheet
ρ_f	1.93 g/cm^3	Experimental by granulometric analysis
ν	0.46	Experimental by DIC technique
φ_m	0.632	Tabulated in [27]

Developed models allow to analyze tensile stresses as well as elastic modulus.

2.5. Yield Strength. A simple model to predict the yield strength as a function of the filler content was proposed by Nicolais and Narkis [28]. The model supposes that the presence of the filler reduces the cross-sectional area, and the load during deformation is carried by the only continuous phase, that is, the matrix. In the case of composites filled with uniformly dispersed spherical particles, the Nicolais and Narkis' equation is expressed as

$$\sigma_{y,c} = \sigma_{y,m}\left(1 - 1.21\varphi_f^{2/3}\right), \quad (5)$$

where $\sigma_{y,c}$ and $\sigma_{y,m}$ are the yield stresses of the composite and of the unfilled polymer, respectively. Equation (5), however, lacks in considering interaction between the particles and the matrix, assuming "no adhesion" therefore, the results often deviate from the predictions [1, 28].

A modification from the previous model was presented by Pukánszky et al. [29], who made some adjusting considerations about the cross-section and came up with the following expression:

$$\sigma_y = \sigma_{y0} \frac{1 - \varphi_f}{1 + 2.5\varphi_f} \exp\left(B \bullet \varphi_f\right), \quad (6)$$

where σ_y and σ_{y0} are the yield stresses of the composite and matrix, respectively.

In this work, Equation (6) was applied in its linearized form:

$$\log\left(\sigma_{y,rel}\right) = \log\left(\frac{\sigma_y\left(1 + 2.5\varphi_f\right)}{\sigma_{y0}\left(1 - \varphi_f\right)}\right) = B \bullet \varphi_f, \quad (7)$$

so that in the semilogarithmic plot of $\log(\sigma_{y,\mathrm{rel}})$ against φ_f, straight lines should be obtained. B value can be acquired by the slope of the fitting line.

(a) (b)

Figure 1: Specimens obtained by injection molding without sprue, before (a) and after (b) tensile test; top down: PBAT, PBAT+5% ZTC, PBAT+10% ZTC, and PBAT+20% ZTC.

In Pukánszky's model, B is an empirical parameter that considers the strength of interactions defined as

$$B = \left(1 + A_f \rho_f l\right) \ln \frac{\sigma_{yi}}{\sigma_{y0}}. \quad (8)$$

Equation (8) features the extension of the interfacial surface (A_f), the thickness (l), and strength (σ_{yi}) of the interphase.

The composition dependance of the tensile properties at break is also discussed. It can be expressed through a modification of Equation (6):

$$\sigma_{B,T} = \sigma_{B,T_0\text{rel}} \lambda^n \frac{1 - \varphi_f}{1 + 2.5\varphi_f} \exp\left(B_b \varphi_f\right), \quad (9)$$

where $\sigma_{B,T}$ and $\sigma_{B,T_0,\text{rel}}$ are the true tensile stress at break of the composite and the corresponding true tensile stress at break of the matrix, respectively. Tensile stress is an engineered quantity that refers to the initial cross-section and does not consider that the cross-section varies during deformation. In the calculation of stress at break, engineered tensile strength σ must be converted into true stress $\sigma_{B,T} = \sigma \bullet \lambda$ as a function of relative elongation $\lambda = L/l_0$, with $L = l_0 + \Delta l$ the actual length and l_0 the initial length of the specimen, respectively. $\sigma_{B,T_0\text{rel}} = \sigma_{B,T_0}/\lambda^n$ is the true tensile stress at break of the PBAT matrix ($\sigma_{B,T_0} = \sigma_0 \bullet \lambda$), where λ^n is a correction factor characterizing the strain hardening tendency happening in the polymer structure during deformation by means of the parameter n [18].

n value was derived from the slope of the last section of the true tensile curve, obtained plotting log (σ_T) vs. log (λ), as a mean value of seven replicates.

Rearranging Equation (9), Equation (10) is obtained and linearized such as in Equation (11):

$$\sigma_{B,T\,\text{red}} = \frac{\sigma_{B,T}\left(1 + 2.5\varphi_f\right)}{\lambda^n \sigma_{B,T_0 rel}\left(1 - \varphi_f\right)} = \exp\left(B_b \varphi_f\right), \quad (10)$$

$$\log\left(\sigma_{B,T\,\text{red}}\right) = B_b \varphi_f. \quad (11)$$

Therefore, comparably to the yield stress, plotting log ($\sigma_{B,T\,\text{red}}$) as a function of φ_f, a straight line was obtained, the slope of which gives the B_b value at break.

B_b is defined analogously to Equation (9) but it can assume a different value from that determined by the yield stress. Usually, both elongation and strength decrease with increasing filler content but sometimes reinforcing effects are observed [1].

As it is clear from the formulation of B, the properties of heterogeneous materials are influenced by many factors, four the main ones: the properties of the single components, the composition, the structure, and the interfacial interactions [16]. In particular, the quality of the interaction is generally measured in terms of strength and thickness of the interphase [30], and in the case of Pukánszky's model, it is indeed given by the value assumed by B.

Pukánszky's and modified Pukánszky's models were applied in the forms of Equation (7) and Equation (11), respectively, to analyze the trend of experimental tensile properties in comparison with the theoretical calculated values and to investigate the extension of the interphase interaction.

2.6. Scanning Electron Microscopy. The microstructure of the materials was investigated through scanning electron microscopy (SEM), performed with a Field Emission Gun SEM (FESEM, Nova NanoSEM 450, FEI company, USA). The samples were prepared by previously breaking the specimens in liquid nitrogen in cross-sectional direction, to have an observable fracture surface as smooth as possible.

3. Results and Discussion

3.1. Tensile Test Characterization. Figure 1 represents the specimens before (a) and after (b) the tensile test.

Already from the casting of the polymer-chloroform solution, it was evident that the ZTC addition influenced the PBAT appearance from a partially clear white to an opaque cream white color even at the lowest concentration of filler.

The stress-strain curves of PBAT and PBAT-based composites are represented in Figure 2. A color scale will be adopted throughout the paper in which to a darker shade corresponds a more loaded composite.

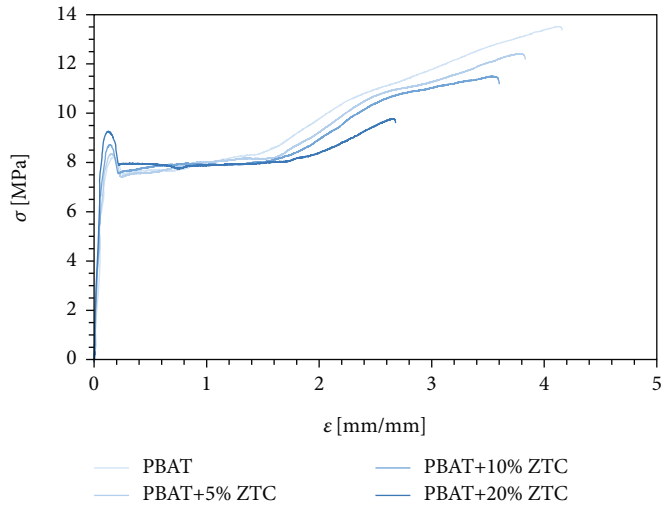

Figure 2: Stress-strain curves of PBAT and PBAT composites obtained by UTT.

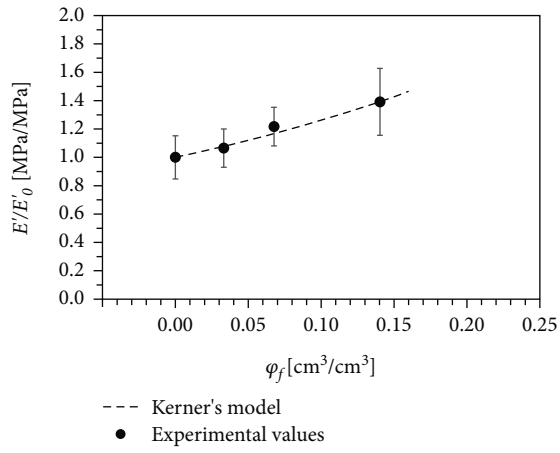

Figure 3: Comparison between experimental Young's moduli of PBAT composites and the corresponding theoretical values, calculated with the Kerner's model.

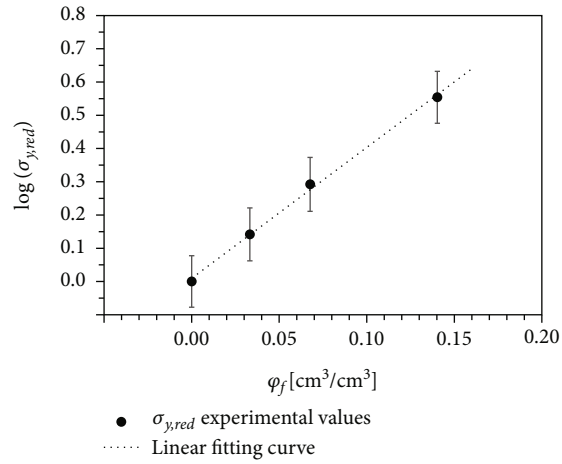

Figure 4: Relative tensile stress at yield, $\sigma_{y,\mathrm{rel}}$, calculated according to the Pukanszky's model, as a function of the ZTC volumetric fraction.

PBAT-ZTC composites proved to be tough materials, with an initial linear elastic section, followed by a yielding peak that corresponds to the beginning of plastic deformation. After yielding, a zone where the stress remains fairly constant corresponds to the propagation of the necking along the whole central section of the specimen, due to the alignment of the polymer chains along the tensile axis. Finally, an increase in the stress values is observed up to the specimen failure.

The ZTC addition shows a reinforcing effect in terms of E and σ_y. In particular, with the increase of filler content, increments up to 44 and 10% are observed for E and σ_y, respectively. Besides, the overall reduction of 27, 33, and 42% of, respectively, σ_B, ε_B, and T can be noted. Numerical values of discussed parameters are shown in Supplementary Table 1.

Increase in E values is mainly due to the addition of a stiffer component compared to the matrix (reference to E_p and E_m can be found in Table 1) [19, 27, 31]. Another commonly reported explanation for this behavior is the mechanical restraint the filler particles create to the polymer chain mobility during tensile conditions [32]. A decrease in flexibility is the main downside mostly obtained in front of the reinforcement.

On the other hand, an important result is the σ_y increase with increasing the filler content, since it is only occasionally obtained [33]. This might be due to the formation of a strong interface layer between the surface of the ZTC and PBAT. Discussion about this last hypothesis will be carried out through the analysis of composite modelling results and SEM images.

3.2. Composite Modelling. The E increase can be modelled by applying Nielsen-Lewis' formulation of Kerner's equation (Equation (4)). According to this model, E can be predicted for composites filled with homogeneously dispersed spherical particles.

In Figure 3, the experimental moduli, expressed as ratio between the composite (E') and the neat polymer (E'_0) values, are compared to the theoretical predicted values.

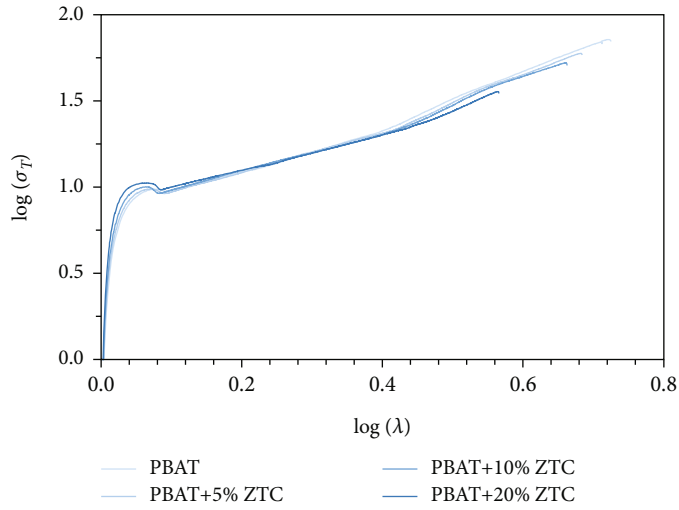

Figure 5: True stress-strain curves of PBAT-ZTC composites.

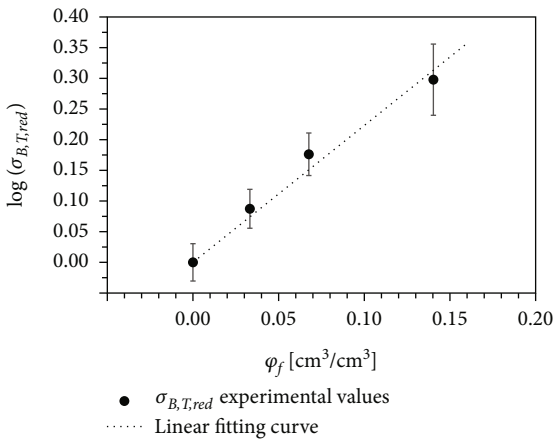

Figure 6: Relative tensile true stress at break, $\sigma_{B,T,\mathrm{red}}$, calculated according to the modified Pukánszky's model, as a function of the ZTC volumetric fraction with linear fit.

Very good correspondence is found between the two series, even at high ZTC concentration. Deviations from Kerner's prediction might happen when filler acts as net points and thus the composite cross-linking increases: higher values of relative modulus are usually obtained compared to those expected by the application of Kerner's model [34]. In such a case, it has been reported that more reliable predictions can be achieved by modelling the E behavior with Halpin-Tsai's equation (Equation (2)), where with increasing the parameter ξ, the difference between experimental and predicted data can be reduced [35].

The reinforcing effect really depends on the characteristics of the filler and matrix. A larger reinforcement is obtained when a stiff filler is added to a flexible matrix, like in elastomers, obtaining an increase in both stiffness and strength [1]. On the other hand, when added to a stiffer matrix, the effect of the reinforcement is less obvious [16]. Concerning the composition, one of the main goals is the realization of composites with the best compromise between reduction of pristine matrix costs and optimization of mechanical properties.

σ_y was analyzed through the application of Pukánszky's model (Equation (7)). In Figure 4 experimental $\sigma_{y,\mathrm{rel}}$ values of PBAT-ZTC composites are shown as a function of φ_f. The slope of the fitting line returns a B value of 4.06 ± 0.12, validating a positive interphase interaction.

Generally, B values characterizing efficient reinforcement are included in a wide range, going from 2 to 15 [16]. To cite some valuable examples taken from recent works on the characterization of biocomposites, B values as extrapolated by Pukánszky's Equation (8) were reported to be equal to 2.10 for poly(lactic acid) (PLA) filled with hemp particles wastes [36] and 2.19 and 3.32 for poly(3-hydroxybutyrate-*co*-hydroxyhexanoate) (PHBH) and poly(3-hydroxybutyrate-*co*-hydroxyvalerate) (PHBV) filled with wine lees wastes, respectively [37].

In other cases, deviation from linearity might occur, and common explanations for this situation consist in structural effects, as the aggregation of the filler, reducing interfacial area and negatively influencing the interaction between phases, up to obtain negative values of B [16, 38, 39].

Being a measurement of the strength of interaction, higher values of B represent a better adhesion between the surface and the matrix, indicating the formation of a stronger interphase layer, with effective stress transfer from the matrix to particles [40]. Vice versa when B assumes low values it denotes poor interaction between matrix and filler, reducing the load-bearing capacity of the cross-section, leading to a decrement of mechanical properties of the composites.

As already introduced, ultimate tensile properties can be modelled in a similar way to yield stress, applying a modification to Pukánszky's model (Equation (11)). Strain hardening is represented by n in the λ^n term. n was calculated considering the slope of the curve section for $\log(\lambda) > 0.5$: a linear fit was applied, obtaining a constant slope of $n = 1.588$.

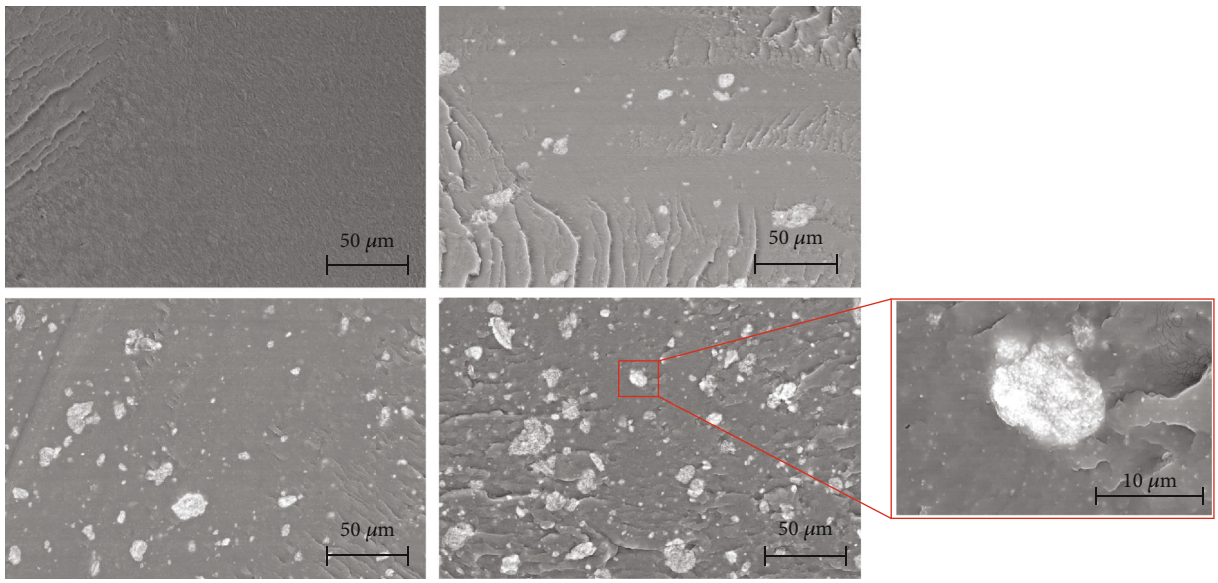

Figure 7: SEM images of PBAT (a), PBAT+5% ZTC (b), PBAT+10% ZTC (c), and PBAT+20% ZTC (d) at a magnification of 1600× and of a single ZTC particle detail at 12000× (e).

True tensile curves, calculated as $\sigma_{B,T} = \sigma \bullet \lambda$, for all the PBAT composites are reported in Figure 5.

Analyzing the graph, analogously to the stress strain curves (Figure 2), a variation in the yielding area is remarkable, alongside a reduction of the tensile parameters at break. In particular, the failure of the materials occurs at lower $\sigma_{B,T}$ values and relative elongation.

In Figure 6, experimental values of $\sigma_{B,T,\text{red}}$ are plotted in a semilogarithmic scale. The slope of the fitting line gives a value of $B_b = 2.23 \pm 0.12$, which is lower compared to the one obtained with the fitting of relative yield stresses. The value achieved is in any case included in the range of values indicating a good degree of interfacial interaction [41], although the trend of σ_y and of $\sigma_{B,T}$, leading to a different behavior in the application of Pukánszky's model, is unclear. For the sake of comparison, B_b value of PLA filled with natural fibers was obtained equal to 2.29 [42], while B_b values for PP filled with carbon fibers, glass fibers, and wood flour revealed to be equal to 4.45, 4.64, and 3.13, respectively [43]. In the latter case, the values are more similar to B obtained in this work for yield stress. Considering previously studied composites made of PBAT filled with calcium-phosphate glass (CPG) microparticles, a value of $B_b = 2.30 \pm 0.08$ was obtained in the application of Pukánszky's model for the stress at break [44].

However, it must be considered that the real $\sigma - \varepsilon$ curves substantially assume the same trend with the increase of the filler content, with a deformation at break that decreases due to the increase in the stiffness of the composite. This detail is not observed in the engineered $\sigma - \varepsilon$ curves (Figure 2), where σ_B seems to have a marked variation at a specific ε.

Increasing in B can be achieved acting on the factors influencing interfacial interaction, defined in Equation (8).

Particle size and size distribution are of fundamental importance, since interphase interaction takes place on the surface area A_f. Hence, the smaller the particle is, the higher the specific area and the larger the reinforcement due to the interphase interactions are. The reinforcing phase is usually added to the matrix in form of micrometric or nanometric particles and fibers. Increasing particle size is expected to negatively affect tensile strength, since large particles tend to debond more easily from the matrix under loading, often leading to premature failure. On the other hand, too small particles could trigger aggregation: when aggregation takes place, the specific surface area decreases, thus causing a reduction of the mechanical properties [1].

Due to the possible difference in chemical nature of polymers and fillers, incompatibility between the phases may arise and cause poor adhesion by drastically decreasing the value of B. In the worst case of zero adhesion between the filler particles and the continuous phase, there is no load transfer to the filler, and the total load is carried by the matrix [29]; furthermore, the load-bearing section decreases with increasing the filler content.

To achieve higher values of filler-matrix adhesion and enhance interphase strength, the surface treatment of the filler, the functionalization of the polymer, and the use of compatibilizers might be considered. Surface treatment modifies both particle/particle and matrix/filler interactions, bringing the properties of the composite to be a combination of the two effects. In the case of cellulose and natural fibers, further chemical modifications might be performed by acetylation, cyanoethylation, peroxide treatment, and silane treatments [40, 45]. Processes of surface modification require careful optimization in terms of both technical and economical point of view, determining the most suitable type and quantity of reagents.

Panaitescu et al. [45] studied the properties of maleated polypropylene (MA-PP) filled with microfibrillated cellulose (MFC) at different concentrations, obtaining a marked increase in tensile modulus and strength when compared to the simple PP-MFC composite system without coupling

agent. Analogously, Nanni et al. [46] obtained enhanced mechanical properties, without a decrease in tensile strength even at high filler concentration, when maleic anhydride was used as coupling agent in PP-spent coffee ground (SCG) systems. Indeed, Pukánszky's B factor was found to be higher compared to simple PP-SCG composites.

Therefore, these results suggested the interfacial bonding improvement, with enhanced stress transfer and more performing mechanical properties. Yang et al. realized polyethylene- (PE-) lignocellulosic materials composites, obtaining analogous results but highlighting that compatibilization with maleic anhydride has a stronger effect on the enhancement of PE properties compared to MA-PP, due to a better wetting [4]. Surface modification of bamboo fibers with NaOH aqueous solution and salinization was performed in the realization of epoxy composites. Increases in tensile strength and elongation at break, compared to the untreated filler-epoxy composite, were obtained in both cases [47]. Metin et al. obtained that silane coupling agents improved interfacial adhesion between filler and matrix in a PP system filled with treated zeolite compared to nontreated particles: both tensile modulus and yield strength were enhanced [38]. Silanization of MFC in PHBH composites also showed to induce a more pronounced reinforcing effect compared to untreated cellulose, due to a better interfacial compatibility [48].

3.3. SEM Characterization. Figure 7 represents SEM images of PBAT (Figure 7(a)) and PBAT-ZTC composites microstructure (Figures 7(b)–7(d)). Homogeneous dispersion of the ZTC within the PBAT matrix with no aggregation nor phase separation is maintained even at the higher filler concentration.

The ZTC particle is characterized by a modulation of its brightness. The bright white areas correspond to the TiO_2 portion of the ZTC, while zein is represented by the lighter shade of grey. The dark grey background is the PBAT matrix.

The formation of an interface between the surface of the filler and the matrix can be hypothesized by the absence of a sharp boundary around the particles and of any kind of phase separation, which would cause the failure of the materials. In fact, a smooth variation in the shades of grey (Figure 7(e)), corresponding to the area where the bonds between the functional groups of the zein and the PBAT chain are formed, can be observed.

4. Conclusions

Polymer composites are designed to enhance the polymer properties. Within this framework, theoretical models represent a promising tool for studying the effect of the addition of a reinforcing component on the tensile properties of the polymer matrix.

In this work, new sustainable composite materials were successfully realized by the addition of different quantities of ZTC to a PBAT matrix and mechanically characterized. Enhancement of stiffness and yield strength, up to 44 and 10%, respectively, was obtained as a function of filler content. Application of Kerner-Nielsen's model returned excellent agreement with the experimental E values, and Pukánszky's models gave values of $B = 4.06 \pm 0.12$ and $B_b = 2.23 \pm 0.12$ for $\sigma_{y,\mathrm{rel}}$ and $\sigma_{B,T}$, respectively. Finally, microstructure of specimen cross-section was investigated by SEM, observing homogeneous dispersion of the filler within the matrix with good adhesion between the phases.

According to the collected results, a strong interface was created between the ZTC particle surface and the PBAT, providing an efficient and adjustable reinforcement of the pristine polymer.

These composites offer a sustainable alternative to non-biodegradable plastics that are normally used and not properly disposed of or recovered. Furthermore, the possibility of property modulation, obtained by suitably varying the filler content, allows to customize the material characteristics to the needs.

Data Availability

Authors can also make data available on request through a data access committee, institutional review board, or the authors themselves. In this case, they should name who should be contacted to request the data (e.g., the ethics or data access committee) and provide appropriate contact details. When authors have used third party data (i.e., from another individual or source) and therefore do not own the data, this source must be credited as appropriate and details of how to access the data should be given.

Conflicts of Interest

The authors declare no conflicts of interest.

Authors' Contributions

Elena Togliatti did the investigation, formal analysis, and writing—original draft. Maria Grimaldi did the investigation. Olimpia Pitirollo did the investigation. Antonella Cavazza did the resources. Diego Pugliese did the investigation. Daniel Milanese did the supervision and writing—review and editing. Corrado Sciancalepore did the conceptualization, methodology, supervision, and writing—review and editing. All authors have read and agreed to the published version of the manuscript.

Supplementary Materials

In the Supplementary data file, the reader can find a table (Supplementary Table 1) reporting the numerical values of the tensile parameters (E, σ_y, σ_B, ε_B, and T), collected through the tensile tests on the PBAT-based composites. *(Supplementary Materials)*

References

[1] J. Móczó and B. Pukánszky, "Polymer micro and nanocomposites: structure, interactions, properties," *Journal of Industrial and Engineering Chemistry*, vol. 14, no. 5, pp. 535–563, 2008.

[2] T. Kijchavengkul, R. Auras, M. Rubino, S. Selke, M. Ngouajio, and R. T. Fernandez, "Biodegradation and hydrolysis rate of aliphatic aromatic polyester," *Polymer Degradation and Stability*, vol. 95, no. 12, pp. 2641–2647, 2010.

[3] J. Jian, Z. Xiangbin, and H. Xianbo, "An overview on synthesis, properties and applications of poly(butylene-adipate-co-terephthalate)–PBAT," *Advanced Industrial and Engineering Polymer Research*, vol. 3, no. 1, pp. 19–26, 2020.

[4] H. -S. Yang, M. P. Wolcott, H. -S. Kim, S. Kim, and H. -J. Kim, "Effect of different compatibilizing agents on the mechanical properties of lignocellulosic material filled polyethylene biocomposites," *Composite Structures*, vol. 79, no. 3, pp. 369–375, 2007.

[5] E. L. Sánchez-Safont, A. Aldureid, J. M. Lagarón, J. Gámez-Pérez, and L. Cabedo, "Biocomposites of different lignocellulosic wastes for sustainable food packaging applications," *Composites Part B: Engineering*, vol. 145, pp. 215–225, 2018.

[6] H. Zhang and S. Sablani, "Biodegradable packaging reinforced with plant-based food waste and by-products," *Current Opinion in Food Science*, vol. 42, pp. 61–68, 2021.

[7] H. Moustafa, C. Guizani, and A. Dufresne, "Sustainable biodegradable coffee grounds filler and its effect on the hydrophobicity, mechanical and thermal properties of biodegradable PBAT composites," *Journal of Applied Polymer Science*, vol. 134, no. 8, article 44498, 2017.

[8] A. S. M. Bashir and Y. Manusamy, "Recent developments in biocomposites reinforced with natural biofillers from food waste," *Polymer-Plastics Technology and Engineering*, vol. 54, no. 1, pp. 87–99, 2015.

[9] J. W. Lawton, "Zein: a history of processing and use," *Cereal Chemistry*, vol. 79, no. 1, pp. 1–18, 2002.

[10] J. -H. Oh, B. Wang, P. D. Field, and H. A. Aglan, "Characteristics of edible films made from dairy proteins and zein hydrolysate cross-linked with transglutaminase," *International Journal of Food Science and Technology*, vol. 39, no. 3, pp. 287–294, 2004.

[11] L. M. Anaya-Esparza, Z. Villagrán-de la Mora, N. Rodríguez-Barajas et al., "Protein–TiO_2: a functional hybrid composite with diversified applications," *Coatings*, vol. 10, no. 12, p. 1194, 2020.

[12] F. L. Gomes de Menezes, R. H. De Lima Leite, F. K. Gomes dos Santos, A. I. Aria, and E. M. M. Aroucha, "TiO_2-enhanced chitosan/cassava starch biofilms for sustainable food packaging," *Colloids and Surfaces A: Physicochemical and Engineering Aspects*, vol. 630, article 127661, 2021.

[13] D. M. Kadam, M. Thunga, G. Srinivasan et al., "Effect of TiO_2 nanoparticles on thermo-mechanical properties of cast zein protein films," *Food Packaging and Shelf Life*, vol. 13, pp. 35–43, 2017.

[14] L. E. Nielsen, "Generalized equation for the elastic moduli of composite materials," *Journal of Applied Physics*, vol. 41, no. 11, pp. 4626-4627, 1970.

[15] T. B. Lewis and L. E. Nielsen, "Dynamic mechanical properties of particulate-filled composites," *Journal of Applied Polymer Science*, vol. 14, no. 6, pp. 1449–1471, 1970.

[16] L. Százdi, B. Pukánszky, G. J. Vancso, and B. Pukánszky, "Quantitative estimation of the reinforcing effect of layered silicates in PP nanocomposites," *Polymer*, vol. 47, no. 13, pp. 4638–4648, 2006.

[17] B. Pukánszky, "Interfaces and interphases in multicomponent materials: past, present, future," *European Polymer Journal*, vol. 41, no. 4, pp. 645–662, 2005.

[18] B. Pukánszky, "Influence of interface interaction on the ultimate tensile properties of polymer composites," *Composites*, vol. 21, no. 3, pp. 255–262, 1990.

[19] J. C. Halpin Affdl and J. L. Kardos, "The Halpin-Tsai equations: a review," *Polymer Engineering and Science*, vol. 16, no. 5, pp. 344–352, 1976.

[20] E. H. Kerner, "The elastic and thermo-elastic properties of composite media," *Proceedings of the Physical Society. Section B*, vol. 69, no. 8, pp. 808–813, 1956.

[21] G. Bourkas, I. Prassianakis, V. Kytopoulos, E. Sideridis, and C. Younis, "Estimation of elastic moduli of particulate composites by new models and comparison with moduli measured by tension, dynamic, and ultrasonic tests," *Advances in Materials Science and Engineering*, vol. 2010, Article ID 891824, 2010.

[22] Y. Zare and K. Y. Rhee, "Effects of critical interfacial shear strength between a polymer matrix and carbon nanotubes on the interphase strength and Pukanszky's "B" interphase parameter," *RSC Advances*, vol. 10, no. 23, pp. 13573–13582, 2020.

[23] Y. Zare, K. Y. Rhee, and S. -J. Park, "Simple models for interphase characteristics in polypropylene/montmorillonite/$CaCO_3$ nanocomposites," *Physical Mesomechanics*, vol. 23, no. 2, pp. 182–188, 2020.

[24] Y. Zare and H. Garmabi, "Analysis of tensile modulus of PP/nanoclay/$CaCO_3$ ternary nanocomposite using composite theories," *Journal of Applied Polymer Science*, vol. 123, no. 4, pp. 2309–2319, 2012.

[25] J. C. Halpin, "Stiffness and expansion estimates for oriented short fiber composites," *Journal of Composite Materials*, vol. 3, no. 4, pp. 732–734, 1969.

[26] A. Lopez-Gil, M. A. Rodriguez-Perez, J. A. De Saja, F. S. Bellucci, and M. Ardanuy, "Strategies to improve the mechanical properties of starch-based materials: plasticization and natural fibers reinforcement," *Polímeros*, vol. 24, no. ESP, pp. 36–42, 2014.

[27] L. E. Nielsen and R. F. Landel, *Mechanical Properties of Polymers and Composites*, CRC Press, Boca Raton, Florida, United States, 1993.

[28] L. Nicolais and M. Narkis, "Stress-strain behavior of styrene-acrylonitrile/glass bead composites in the glassy region," *Polymer Engineering and Science*, vol. 11, no. 3, pp. 194–199, 1971.

[29] B. Turcsányi, B. Pukánszky, and F. Tüdős, "Composition dependence of tensile yield stress in filled polymers," *Journal of Materials Science Letters*, vol. 7, no. 2, pp. 160–162, 1988.

[30] Y. Zare, "New models for yield strength of polymer/clay nanocomposites," *Composites Part B: Engineering*, vol. 73, pp. 111–117, 2015.

[31] B. Pukánszky, B. Turcsányi, and F. Tüdős, "Effect of interfacial interaction on the tensile yield stress of polymer composites," in *In Interfaces in Polymer, Ceramic and Metal Matrix Composites*, pp. 467–477, Elsevier, 1988.

[32] R. Taurino, C. Sciancalepore, L. Collini, M. Bondi, and F. Bondioli, "Functionalization of PVC by chitosan addition: compound stability and tensile properties," *Composites Part B: Engineering*, vol. 149, pp. 240–247, 2018.

[33] P. Reichert, H. Nitz, S. Klinke, R. Brandsch, R. Thomann, and R. Mülhaupt, "Poly(propylene)/organoclay nanocomposite formation: influence of compatibilizer functionality and organoclay modification," *Macromolecular Materials and Engineering*, vol. 275, no. 1, pp. 8–17, 2000.

[34] G. Barrera, C. Sciancalepore, M. Messori, P. Allia, P. Tiberto, and F. Bondioli, "Magnetite-epoxy nanocomposites obtained by the reactive suspension method: microstructural, thermomechanical and magnetic properties," *European Polymer Journal*, vol. 94, pp. 354–365, 2017.

[35] M. Degli Esposti, F. Bisi, V. Righi et al., "Epoxy resin/TiO_2 nanocomposites prepared by the *reactive suspension method*: dynamic-mechanical properties and their prediction by theoretical models," *Materials Today Communications*, vol. 31, p. 103347, 2022.

[36] D. Battegazzore, A. Noori, and A. Frache, "Natural wastes as particle filler for poly(lactic acid)-based composites," *Journal of Composite Materials*, vol. 53, no. 6, pp. 783–797, 2019.

[37] A. Nanni and M. Messori, "Effect of the wine lees wastes as cost-advantage and natural fillers on the thermal and mechanical properties of poly(3-hydroxybutyrate-co-hydroxyhexanoate) (PHBH) and poly(3-hydroxybutyrate-co-hydroxyvalerate) (PHBV)," *Journal of Applied Polymer Science*, vol. 137, no. 28, p. 48869, 2020.

[38] D. Metin, F. Tihminlioğlu, D. Balköse, and S. Ülkü, "The effect of interfacial interactions on the mechanical properties of polypropylene/natural zeolite composites," *Composites Part A: Applied Science and Manufacturing*, vol. 35, no. 1, pp. 23–32, 2004.

[39] A. Kiss, E. Fekete, and B. Pukánszky, "Aggregation of $CaCO_3$ particles in PP composites: effect of surface coating," *Composites Science and Technology*, vol. 67, no. 7-8, pp. 1574–1583, 2007.

[40] J. George, M. S. Sreekala, and S. Thomas, "A review on interface modification and characterization of natural fiber reinforced plastic composites," *Polymer Engineering and Science*, vol. 41, no. 9, pp. 1471–1485, 2001.

[41] D. Kun and B. Pukánszky, "Polymer/lignin blends: Interactions, properties, applications," *European Polymer Journal*, vol. 93, pp. 618–641, 2017.

[42] G. Faludi, G. Dora, K. Renner, J. Móczó, and B. Pukánszky, "Biocomposite from polylactic acid and lignocellulosic fibers: structure-property correlations," *Carbohydrate Polymers*, vol. 92, no. 2, pp. 1767–1775, 2013.

[43] R. Várdai, T. Lummerstorfer, C. Pretschuh et al., "Comparative study of fiber reinforced PP composites: effect of fiber type, coupling and failure mechanisms," *Composites Part A: Applied Science and Manufacturing*, vol. 133, p. 105895, 2020.

[44] C. Sciancalepore, E. Togliatti, A. Giubilini et al., "Preparation and characterization of innovative poly(butylene adipate terephthalate)-based biocomposites for agri-food packaging application," *Journal of Applied Polymer Science*, vol. 139, no. 24, p. 52370, 2022.

[45] D. M. Panaitescu, D. Donescu, C. Bercu, D. M. Vuluga, M. Iorga, and M. Ghiurea, "Polymer composites with cellulose microfibrils," *Polymer Engineering and Science*, vol. 47, no. 8, pp. 1228–1234, 2007.

[46] A. Nanni, M. Colonna, and M. Messori, "Fabrication and characterization of new eco-friendly composites obtained by the complete recycling of exhausted coffee capsules," *Composites Science and Technology*, vol. 222, p. 109358, 2022.

[47] T. Lu, M. Jiang, Z. Jiang, D. Hui, Z. Wang, and Z. Zhou, "Effect of surface modification of bamboo cellulose fibers on mechanical properties of cellulose/epoxy composites," *Composites Part B: Engineering*, vol. 51, pp. 28–34, 2013.

[48] A. Giubilini, C. Sciancalepore, M. Messori, and F. Bondioli, "New biocomposite obtained using poly(3-hydroxybutyrate-co-3-hydroxyhexanoate) (PHBH) and microfibrillated cellulose," *Journal of Applied Polymer Science*, vol. 137, no. 32, p. 48953, 2020.